A REVIEW OF FLIGHT-TO-WIND TUNNEL DRAG CORRELATION

Edwin J. Saltzman* and Theodore G. Ayers**
NASA Dryden Flight Research Center
Edwards, California

Abstract

The correlation of flight and wind-tunnel data has been the subject of considerable discussion for several decades. It is safe to say that the success of these efforts has varied from complete failure to successful, depending upon the class and complexity of the configuration and the performance level for which it was designed.

This paper reviews attempts to correlate flight and wind-tunnel-model drag or drag-related data from the mid-1940's to the 1970's. The discrepancies between the model and flight drag data considered have much in common, irrespective of their decade of origin. The discrepancies primarily involve Reynolds number and wall interference effects. Less prominent are sting support effects and, in the case of a large flexible airplane, the inability of the model to simulate the surface deflections for longitudinal trim.

In two instances where relatively simple, clean, rigid configurations were tested, the model-to-flight drag correlation confirmed the T' method of extrapolating model compressible turbulent friction drag for Reynolds number effects. A unique wind-tunnel-to-flight correlation of turbulent skin friction that used the same hollow cylinder for both types of tests also confirmed the T' method.

The authors' observations concerning the subject review lead them to believe that the new cryogenic facilities will improve the fidelity of model simulation of full-scale flight flow phenomena.

Introduction

Most increments of improvement in aircraft performance have their origin in model testing, most often wind-tunnel models. This approach, which was even used at times by the Wright brothers, remains a key element in the development of configurations that are more efficient, have more endurance, or perform over a more extensive range of speed or lift.

Though the community of aircraft designers must depend heavily upon model data and theory, their confidence in each should occasionally be bolstered by a flight demonstration to evaluate whether ground-based tools can indeed simulate real world aerodynamic phenomena. Over the years, as the increments of improvement in performance have become smaller and aircraft development costs have risen, casual model-to-flight drag comparisons have sometimes given way to very comprehensive correlation efforts involving precise sensors, the careful control of variables, and great attention to detail on behalf of both the tunnel experimenters and their flight counterparts.

Examples of both the somewhat casual model-to-full scale flight drag comparisons and the more comprehensive correlations of local aerodynamics are given in this paper, which reviews some of the flight-to-wind tunnel and flight-to-flight data comparisons that have been made within the experience or the cognizance of the authors. The review reaches back to shortly after World War II, when compressibility effects became a commonly recognized barrier to further increases in aircraft speed. From that period, the review progresses forward to relatively recent flight experience.

This paper should not be considered historical; rather, it is a somewhat narrow review of flight and wind-tunnel-model drag tests by two engineers whose concerns include the business of flight testing and flight research. It is intended for this review to provide a degree of insight into situations where model testing has been adequate and those where, conversely, the simulation of full-scale flight flow conditions has been inadequate. Methodology is not emphasized, although it is mentioned occasionally when it gives perspective. Primary emphasis is on drag components influenced by transonic conditions over the external surfaces of a variety of configurations; however, wind-tunnel and flight examples of the variation of compressible turbulent skin friction with Reynolds number are also included.

Symbols

A	cross-sectional area
C_D	drag coefficient, D/qS
C'_D	$= C_D - C_{D_b} - C_{D_\beta}$
C_{D_b}	base drag coefficient, D_{base}/qS
C_{D_β}	boattail drag coefficient
ΔC_D	$= C_D - C_{D_{M=0.9}}$
C_f	local turbulent skin friction coefficient
C_L	lift coefficient, L/qS
$C_{N_{wp}}$	normal force coefficient of wing panel
C_p	pressure coefficient, $\frac{p_\ell - p}{q}$
D	drag
L	lift
ℓ	length of body or fuselage
M	Mach number, free stream unless otherwise indicated

*Aerospace Engineer.
**Chief, Aeronautics Branch, Member AIAA.

M_D	drag divergence Mach number, $\Delta C_D/\Delta M = 0.1$
p	free-stream static pressure
$\sqrt{\bar{p}_s'^2}$	average root-mean-square pressure fluctuation amplitude
q	dynamic pressure, $0.7M^2p$
R	Reynolds number, $\frac{U \cdot \ell}{\nu}$
S	wing reference area
T	temperature
T'	reference temperature
t/c	wing thickness-to-chord ratio
U	free-stream velocity
x/c	wing-chord location
α	angle of attack
δ_a	aileron deflection
δ_e	elevon deflection
Λ	wing sweep angle
ν	kinematic viscosity

Subscripts:

e	edge conditions
ℓ	local
s	static pressure at cone surface
t	total or stagnation value
w	wall
x	distance from leading edge of cylinder
0	zero lift
∞	free-stream conditions

Superscripts:

-	incompressible
'	reference temperature method (also called T' method)

Abbreviated Wind Tunnel Names

UPWT	Unitary Plan Wind Tunnel, NASA Langley Research Center
16 Ft. TT, 16' TT	16-Foot Transonic Tunnel, NASA Langley Research Center
8 Ft. TT - CAL	8-Foot Transonic Tunnel, Calspan Corp.
8 Ft. TPT, 8' TPT	8-Foot Transonic Pressure Tunnel, NASA Langley Research Center

Drag Divergence Mach Number

At the beginning of World War II most bombers flew at speeds not much over 200 mph, and the fighters could reach speeds of approximately 325 mph in level flight. By the end of the war some bombers could attain the fighter speeds of only 5 or 6 years earlier, the fastest propeller-driven fighters could reach 500 mph, and the earliest jet fighters were able to go about 50 mph faster. Thus, over a span of about 7 years fighter aircraft advanced from flow conditions which were predominantly incompressible to what became known as the drag divergence Mach number, M_D.

During the early to mid-1940's few wind tunnels were designed for obtaining transonic data, so several ingenious methods were developed for obtaining data through the speed-of-sound region. Three such methods are represented by cross-hatched bars in Figure 1, obtained from Reference 1. Also shown in Figure 1 is the gap in theory and wind-tunnel experience as of early 1947 at transonic Mach numbers and the maximum Mach number achieved in full-scale flight.

Through the falling-body, wing-flow, and rocket model techniques, which are described briefly in Reference 1, a body of transonic data developed; however, the unknown factors in transonic aerodynamics were considerably more numerous than the known. Because of the unknown Reynolds number effects for all of the experimental methods being used, and because it was uncertain how model support and tunnel wall interference effects were influenced by compressibility, it was believed that some full-scale flight data near the speed of sound would be required to evaluate the existing testing techniques, data, and theory.

An Early Experiment

An early effort to compare the onset of transonic effects on both an accurate model and a full-scale airplane was reported in Reference 2. In this experiment the P-51B airplane was used as the test configuration. Great care was taken in both the flight and the wind-tunnel-model portions of the experiment.

The propeller (a significant modeling problem) was removed from the full-scale airplane, which was then towed to an altitude of about 28,000 feet and released. The pilot then put the aircraft into a dive to achieve high speeds. The especially smoothed, sealed, propellerless, waxed airplane is shown in Figure 2. The model, which is of one-third scale and constructed with great attention to detail, was tested in the then relatively new 16-foot high-speed tunnel at the NACA Ames Laboratory. The drag results from both the wind tunnel and flight are shown in Figure 2. The authors of Reference 2 considered the flight and model drag levels and the drag divergence Mach number to "show satisfactory agreement," thus increasing confidence in the fidelity of the flow characteristics over accurately formed models in a quality wind tunnel. The authors also noted that the flight drag coefficients were considerably larger than the wind-tunnel-model values for comparable lift coefficients during the pull-out from the dive, a matter to be recalled later in this paper.

It is also worthy of comment that these flight lift and drag data were among the earliest obtained by the accelerometer method, thus representing a pioneering effort in obtaining what was referred to during the 1970's as dynamic performance data. During the same experiment, the more traditional force method, which is related to the energy method was also applied, and in reporting the results it was alleged that the force method produced "absurd results" because of the difficulty of accurately determining the slope of the airspeed-time curve during high-speed dives. This observation is consistent with the experience reported in References 3 and 4, where these methods are compared. Thus, the accelerometer method became a trusted, easily applied technique; it has been used for even some of the most recent research aircraft.

Through the Speed of Sound With Unswept Wings

During the last 2 years of World War II, both the U.S. Army and the U.S. Navy became interested in designing airplanes especially to explore the Mach number region near the speed of sound. With the technical advice of NACA, each organization financed the construction of an unswept-wing single-place monoplane. The Navy's D-558-I airplane was turbojet powered; the Army's X-1 (originally the XS-1) was rocket powered and launched from a modified B-29 bomber, which permitted the X-1 to begin powered flight at an altitude of about 25,000 feet. It was expected that from this altitude the X-1 would have sufficient total impulse to reach sonic velocity.

The X-1 number 1 (Fig. 3), which had an 8-percent-thick wing, became the first manned airplane to exceed the speed of sound. Figure 3 shows a section of the airspeed-altitude recording which documented the first in-flight Mach jump. As can be seen by the time scale, sonic velocity was exceeded for an interval on the order of 17 seconds.

Because the companion aircraft, X-1 number 2, had a 10-percent-thick wing, a comparison of the transonic drag data from the two aircraft offered a chance to observe the effect of wing thickness on drag divergence Mach number in flight. As can be seen in Figure 4(a), the thicker wing caused drag divergence to occur at a Mach number about 0.06 lower than the 8-percent-thick wing for a lift coefficient of 0.4. At a lift coefficient of 0.2 the difference in M_D was about 0.03. Figure 4(b) compares the same 10-percent-thick wing data with corresponding 1/16-scale-model results, and the drag divergence Mach numbers agree within about 0.015. These summary power-off, or coasting, flight and wind-tunnel-model data were originally reported in References 5 to 7, and some earlier power-on flight results were reported in Reference 8.

It may be of interest, while discussing the first manned airplane to exceed sonic velocity, to include the first supersonic drag polar obtained in flight. These data are shown in Figure 5. Because no wind-tunnel-model data were available for the thinner winged airplane, these flight data cannot be compared with model results.

Delta Wings

New configurations were developed and flown in rapid succession during the early and mid-1950's, and for reasons of safety, the emphasis in the flight testing was on handling qualities, stability and control, and load distribution. Usually, however, the instrumentation was sufficient to permit lift and drag data to be obtained as well. Though wind-tunnel-model data were not available for every configuration, flight-to-model and flight-to-flight comparisons could be made often enough to maintain confidence in wind-tunnel-derived performance increments resulting from incremental configuration changes. An example of how periodic model and flight testing reinforced each other concerns the XF-92A and YF-102 airplanes. Both airplanes had 60° delta wings and 60° delta tails. The former had a 6.5-percent-thick wing,[9] and the latter had a 4-percent-thick wing.[10] Figure 6 shows photographs of the airplanes and the variation, for each, of drag coefficient with Mach number. The drag divergence Mach number is about 0.03 higher for the YF-102 configuration, which had the thinner wing, and the wave drag increment is about two-thirds of that for the thicker wing. The YF-102 model experienced drag divergence very close to the full-scale airplane but also shows evidence of transonic drag creep at speeds below drag divergence. Wind-tunnel-model results are available for only one of the configurations, that is, the YF-102.

Swept Wings

The somewhat unorthodox Bell X-5 research airplane began flying in mid-1951. The wing sweep of this airplane could be varied in flight from 20° to 59°. The wings also translated fore and aft as wing sweep changed in order to maintain an acceptable relationship between the center of gravity and the aerodynamic center.

This rather chubby airplane clearly showed how increasing wing sweep delayed the effects of compressibility; in tests of both the full-scale aircraft in flight and of a model in a relatively sophisticated slotted-throat tunnel,[11-14] it also revealed how compressibility affected the measurement of drag at speeds immediately adjacent to that of sound. The results are shown in Figure 7, where it is evident that the 59° wing sweep configuration undergoes drag divergence at a Mach number about 0.03 higher than the 45° wing sweep configuration, and the 59° wing sweep wind-tunnel and flight values of drag divergence Mach number agree. Even though the flight and model data for 59° of wing sweep coincide for drag divergence, there is a 12 percent difference in drag coefficient between the two sources of data at Mach 1.0. This illustrates the increasing difficulty of defining drag coefficient very near a Mach number of 1, both in the wind tunnel and in flight. In view of the agreement at the drag divergence Mach number, the present authors suspect that at Mach 1 the aft portions of the model fuselage did not undergo the same flow conditions as the airplane.

Transonic Drag Rise and the Area Rule

A revolutionary concept in the design of supersonic airplanes was developed during 1951 by Richard T. Whitcomb and his co-workers at the NACA Langley Aeronautical Laboratory. The discovery was based on the premise that "near the speed of sound the zero-lift drag rise of a wing-body configuration generally should be primarily dependent on the axial development of the cross-section areas normal to the airstream."[15] The data supporting this principle showed that the transonic drag increment was virtually

the same for a wing-body combination as for a body alone which had the same cross-sectional area development, that is, an equivalent body.

The excellent simulation of the wing-body transonic drag rise increment (wave drag) by the equivalent body analogy led rather naturally to the design principle of smoothing the area development. This was done by reducing the surface slopes of the entire aircraft (both the area growth and, past the maximum value, the area decay) through judicious lengthening, indenting, and volume addition.

A well known application of this smoothing process, popularly known as the area-rule, was the F-102A airplane. The F-102A and the prototype YF-102, which needed the smoothing, are shown in Figure 8 in views that reveal both the fuselage indenting and the aft located added volume. Figure 8 also shows plots of the area development for each.

Figure 9 shows the transonic drag rise increment of both aircraft as obtained in full-scale flight.[16] Also shown are similar data from pairs of 1/5-scale rocket-launched models, 1/20-scale wind-tunnel models, and 1/60-scale equivalent bodies.

The data from the several sources demonstrate the effectiveness of the area smoothing process and the adequacy of the equivalent body toward the simulation of wave drag for a complete wing-body configuration.

The relatively smaller wave drag difference between the two 1/5-scale models, particularly at Mach numbers above 1.0, is believed to be caused by relatively smaller differences in the afterbody geometry for this pair of models as compared to the other model pairs.

Reynolds Number Effects

Viscous drag data obtained almost 200 years ago (actually 1796 to 1798) show that scale and velocity affect skin friction;[17] and NACA airfoil research of the 1930's and 1940's revealed the advantages of maximizing laminar flow.[18] However, during the earliest years of transonic wind-tunnel and flight testing, Reynolds number effects and the friction component of drag were not given much attention for fighter configurations. This would seem to be confirmed by the fact that the wind-tunnel tests reported in References 7, 13, and 15, dealing with the X-1, the X-5, and Whitcomb's early transonic drag-rise experiments, did not use, or made no mention of, grit or wires to fix the location of boundary-layer transition. This was probably because the transonic drag increments attributable to thickness, sweep, and aspect ratio were large in comparison to the Reynolds number effects.

Whitcomb, however, realized during his drag-rise experiments that the equivalent-body principle provided less fidelity when applying fuselage indenting than for his other applications, and he suggested that boundary-layer effects not accounted for in designing the indentation may have been the cause.[15] In any event, the soon-to-occur rush of wind-tunnel-model testing on the various Century-series interceptor airplanes initiated the use of boundary-layer trip devices for simulating the viscous drag of these configurations.[19,20] Thus, viscous effects received increasing attention relative to high-speed interceptors, in that a Reynolds number extrapolation was now sometimes made to wind-tunnel-measured drag data in order to obtain a better prediction of the full-scale performance. Such extrapolations were previously routine for the slower and larger bomber and transport configurations, for which long range and endurance were of more importance than speed and agility.

Friction Drag

The first time the NACA High Speed Flight Station related the measured full-scale drag of an airplane to model data modified by a turbulent boundary-layer extrapolation of skin friction for Reynolds number differences was during the correlation of flight and wind-tunnel data for the YF-102 airplane. This airplane was appropriate because the model had excellent geometric fidelity and had flow-through inlets and also because the basic configuration was simple (no variable inlets or complex exhaust nozzles). In addition, the full-scale airplane had aerodynamically clean surfaces, was structurally rigid, and was well instrumented for measuring thrust and drag.

The results of the correlation of the YF-102 model data and the full-scale flight data for Mach 0.8[10] are shown in Figure 10 along with the flat-plate turbulent-boundary-layer extrapolation of the model data using the Sommer and Short T' method.[21,22]

The same methods provided a good extrapolation at supersonic speeds for the X-15 configuration (Fig. 10).[23,24] This airplane had some of the advantages mentioned with respect to the YF-102, such as structural stiffness and simplicity of configuration, and because it was rocket powered the configuration had the added advantage of having no inlets to simulate. Furthermore, the flight data could be obtained during coasting flight, thereby avoiding the uncertainties involved in measuring thrust. The configuration's large base was a problem, however, because the model and full-scale base pressures did not agree, primarily because of wind-tunnel sting effects. Therefore, the base drag had to be subtracted from the zero-lift drag for each data source before a meaningful correlation resulted. This procedure, although it achieved the immediate goal, is not really a solution to the problem of sting effects on afterbody pressure, however, and this approach to avoiding base drag discrepancies can only be used when both flight and model data are available. Figure 11 shows that a major portion of the zero-lift drag of the X-15 consisted of base drag, especially for Mach numbers below 2.

While these model and flight results for the YF-102 and X-15 configurations confirm a commonly used variation of compressible turbulent skin friction with Reynolds number, more direct flight and wind-tunnel experimental support is now available. In a unique cooperative effort between wind-tunnel and flight research teams, a hollow cylinder about 17 inches in diameter and 120 inches long was used to obtain turbulent skin friction data in both environments.[25,26] The flight data were obtained with the cylinder mounted beneath a YF-12 airplane, and the wind-tunnel results for the cylinder were from the NASA Langley Unitary Plan Wind Tunnel. The results, shown in Figure 12, indicate that skin friction balance data obtained in flight and from the wind tunnel are in good agreement, and both data sources confirm the Karman-Schoenherr variation of turbulent skin friction with Reynolds num-

ber. The range of Reynolds number obtained in flight was achieved through the differences in wall temperature for the two data points.

Boattail Drag, An Occasional Modeling Problem

The aforementioned favorable correlations of the YF-102 and X-15 flight data with the extrapolated wind-tunnel-model results were made easier by the relatively small boattail angles and boattail area of these configurations. For aircraft with large boattail angles or area, or both, the preceding method of extrapolation for Reynolds number effects would probably be less successful because of the inability to simulate the location of flow separation.

The M-2/F-3 lifting body vehicle is a good example of this problem.[27] The configuration has a large boattail area with relatively large boattail angles (Fig. 13(a)). When the same extrapolation procedure that was applied to the YF-102 is applied to the M-2/F-3 (Fig. 13(b), top) the wind-tunnel drag level appears to agree with the flight drag level after the wind-tunnel drag is adjusted to the flight Reynolds number. However, the wind-tunnel-model base drag values did not simulate the flight base drag values, and the M-2/F-3 base area is quite large. Therefore, if the comparison is made with the base drag subtracted (lower portion of Fig. 13(b)), as was done with the X-15, there occurs a disagreement of approximately 15 percent between the extrapolated drag level and the flight results. The fortuitous circumstance wherein base drag and boattail drag differences cancelled each other is believed to be due to the difference in the location of flow separation on the full-scale and model boattail areas.

In the case of the M-2/F-3 configuration, the model boundary layer would be expected to be disproportionately thick because of the lower model Reynolds numbers. Separation would, therefore, occur at a different location over the boattail region than on the full-scale vehicle. In addition, model support and wall reflection effects are likely to modify the pressure over the base and the aft sloping surfaces.

Wall Interference and Reynolds Number Effects

Large Flexible Supersonic Configuration

The large delta-winged XB-70 airplane underwent extensive flight testing during the late 1960's with very comprehensive instrumentation on board for measuring thrust and drag.[28] After the flight tests a rigid 0.03-scale model of the airplane was made to be representative of the steady-state flexible aircraft at Mach 2.53. The wind-tunnel model was tested at 14 Mach number/lift combinations corresponding to conditions which were recorded during steady-state flight tests.[29] Another part of this joint effort between NASA Centers was provided by a team from the Langley Research Center, which extrapolated the wind-tunnel-model results of Reference 29 to the previously flown full-scale flight conditions. Predictions were made of surface deflection effects, inlet spillage, the effects of the boundary-layer trips, Reynolds number effects on skin friction, propulsion system effects, roughness, leakage, interference, and flexibility, and the model base drag was subtracted in favor of flight-measured values. This procedure is reported in Reference 30, and the resulting correlation with the flight data is reported in Reference 31.

Comparisons from Reference 31 are shown in Figure 14 for the Mach number for which the model was shaped (Mach 2.53) and for Mach 1.18. The model results for the higher Mach number are within 5 percent of the flight drag coefficients for the 1g conditions ($C_L \approx 0.1$) despite the fact that the prediction of elevon trim was about 2° off and that the angle of attack required to generate a specific lift coefficient was underpredicted. For Mach 1.18 the model-extrapolated drag is lower than the full-scale flight drag on the order of 10 percent. Corresponding model data at Mach 1.06 (not included here) were about 27 percent lower than the flight drag coefficients. These discrepancies for Mach numbers of 1.18 and 1.06 may represent wall interference effects on apparent required trim deflections. However, when extrapolated model drag values were adjusted to account for flight-measured trim values, about one-third of the drag discrepancy remained for level flight lift conditions. The uncertain effects of flexibility may be a significant part of the remaining drag discrepancy.

Shock/Boundary-Layer Interaction as a Modeling Problem

The mid-1960's saw a renewed interest in the transonic regime. The introduction of the modern jet airliner and visions of efficient supersonic flight generated considerable research at transonic Mach numbers. It was also during this time that unanticipated problems were encountered which adversely affected performance. One of the better known examples was the large discrepancy observed in the wing shock wave location (Fig. 15) between the wind-tunnel and flight data obtained for the Lockheed C-141 transport aircraft at transonic Mach numbers.[32] The possible effect of this discrepancy on the satisfactory prediction of loads, stability, and performance of aircraft of this type provided the impetus for new studies to resolve the differences.

The results from Reference 32 and the new studies indicated that the disproportionate boundary-layer thickness at the model wing trailing edge was the parameter primarily responsible for determining the shock wave location and the resulting pressure distribution. Additional research by Blackwell[33] led to the establishment of a boundary-layer scaling criterion for airfoils with different pressure distributions. This criterion was used extensively in the development by Whitcomb and his associates at Langley of the NASA supercritical airfoil and its subsequent application to aircraft wings.

The Supercritical Wing

The relative boundary-layer thickness criterion described in Reference 33 was indeed an important tool in providing an adequate simulation on the subscale model of the location and strength of the aft shock on the wing upper surface. The simulation was sufficiently reliable to provide a prediction of the drag divergence Mach number at the design lift coefficient. As shown in Figure 16,[34] the drag rise occurred a little less than 0.01 lower in Mach number in flight than for the model in the Langley 8-foot wind tunnel after base and boattail drag for each were subtracted. Considering how close the drag rise is to Mach 1, the simulation is considered to be rather good; however, the size of the model for the wind tunnel was sufficient to cause discrepancies which, as would be expected, grew larger as Mach 1 was approached.

An example of this may be seen in Figure 17, where the pressure distribution for the wing panel is shown for both the model and the airplane in flight.[35] Figure 17 shows that the upper surface second-velocity peaks are greater in magnitude and occur farther aft in flight than on the model. In Reference 35 Whitcomb states that the discrepancy occurs because the model airfoil shape was tuned in an environment affected by the wind-tunnel wall. This occurred in spite of the model-to-test section blockage-ratio's being near the generally accepted value of 0.005 (it was actually 0.0056) as the test conditions were pushed closer to sonic velocity.

The Data Comparisons in Retrospect

A Restatement of the Data Comparisons

A review of the data we have considered shows a number of conditions that can lead to disappointing model-to-flight comparisons. A list of what we have seen appears in Table 1.

The main sources of these discrepancies, all of which occur at transonic speeds, have to do with the following:

- Sting-support interference effects
- Disproportionate boundary-layer (Reynolds number) effects
- Wall interference effects

Sting Support Effects

Sting support effects are not great obstacles for many configurations, and where these effects are important, alternate means of support may sometimes alleviate the problem. There are also special cases when the sting support effect can at least be isolated by subtracting the base drag, as was done for the X-15 and the XB-70, although admittedly this can be done only for cases where the flight base pressure values are already known.

Reynolds Number Effects

The disproportionately thick model boundary layer can in some cases be accommodated through the approach discussed in Reference 33 and as applied by Whitcomb during the F-8 supercritical wing model research. Whitcomb acknowledged that wall interference effects were an added factor that partially invalidated his efforts to deal with the disproportionate boundary layer. More will be mentioned about this matter in a following section.

From the standpoint of the wind-tunnel researcher, perhaps the most promising solution to the disproportionate boundary-layer problem is offered by the various cryogenic facilities which will soon be operational. One of these, the National Transonic Facility (NTF)[36-38] will for some cases provide chord Reynolds numbers of 120 million, and it has the potential to test aeroelastic and Reynolds number effects separately by varying one factor while holding the other constant. The NTF should go a long way toward alleviating model-to-flight discrepancies like those discussed herein.

Wall Interference Effects

The problem of wall interference effects which Whitcomb encountered encouraged him to initiate a new research effort to better understand the problem at Mach numbers very close to 1. A major part of this research involved the testing of various supercritical bodies of revolution, differing only in size, in the Langley 8-Foot Transonic Pressure Tunnel and 16-Foot Transonic Tunnel to assess blockage effects. Finally, carefully controlled interference-free data, for comparison with the wind-tunnel data, were obtained by using a variation of the old falling-body technique of the 1950's. The results of this research are reported in References 39 and 40. A summary of the incremental drag data reported in Reference 39 for the configuration used in the falling-body and wind-tunnel tests (Fig. 18) demonstrates the interference effects of wind-tunnel walls. While wind-tunnel wall interference was not a new discovery, the results of References 39 and 40 were significant in providing quantification of such effects. Whereas a value of blockage ratio of 0.0050 was generally accepted as sufficiently low to avoid significant wall interference effects, Figure 19 shows this not to be the case. This finding is, of course, consistent with the previously shown results from the F-8 supercritical wing wind tunnel-to-flight comparison of chordwise wing pressure distribution. Figure 19, which shows transonic creep Mach number as a function of blockage ratio, provides experimental evidence that transonic creep Mach number may be the earliest indication of wind-tunnel wall interference near Mach 1.0.

Alternatives for the Flight Researcher

We have mentioned some of the special efforts that the wind-tunnel researchers have made to solve some of the modeling and flow simulation problems discussed herein. Their counterparts in flight research have also had to use special means on certain kinds of tasks.

One of the most effective devices has been the local aerodynamics approach, where the aerodynamic phenomena for a single component are defined, in contrast to defining the performance of an entire airplane.

The definition of the base drag of the X-15, the wing pressure distribution for the F-8 supercritical wing, and the skin friction data from the YF-12 hollow cylinder, which have been discussed, are examples of this approach. Another such local aerodynamics experiment, which involved both flight and wind-tunnel researchers, is described in the following section.

The 10° Cone Experiment

Although the effect of blockage can be alleviated through careful attention to model size, and the NTF and other cryogenic tunnels can reduce model size while achieving relatively high chord Reynolds numbers, there still remains the problem of wind tunnel-induced noise. A unique wind tunnel-to-flight correlation effort addressing this problem has been conducted by NASA's Dryden Flight Research Center and the U.S. Air Force Arnold Engineering Development Center.

A precision 10° cone was first used as a test configuration in 23 wind tunnels (including those in three European countries). The same cone was then flown on an F-15 airplane (Fig. 20(a)) at Dryden over

a range of Mach number and altitude conditions. The resulting significantly higher disturbance levels measured in the wind tunnels are shown in Figure 20(b)[41]. The same cone will probably be used to evaluate the flow quality of the NTF when it becomes operational.

One Last Look Back

Despite the number of aircraft and the variety of configurations discussed herein, this review is quite narrow. Transonic conditions have received most of the attention; subsonic cruise has been omitted. In addition, any comparison of the model and flight inlet and exhaust nozzle components of drag, which is discussed in several excellent works, including References 42 to 45, had to be omitted. It may be appropriate to compile an analogous review of the propulsion-airframe components of drag after propulsion-related drag can be tested in the NTF.

At this juncture it is probably appropriate to again study Figure 1, that is, to review the range and sources of aerodynamic knowledge as of early 1947, and to consider how differently one would draw such a figure today. We can all agree that the horizontal bar representing flight experience should now extend far to the right to entry speeds[46] and that wind-tunnel research and theory also now extend to corresponding speeds. Within the transonic Mach number range considered in Figure 1, however, and considering the problems discussed thus far in this paper, it is questionable whether the horizontal bars for the wind tunnels and theory can legitimately be changed more than a very little relative to the reliable prediction of full-scale flight drag. This is even the case for configurations that are rather ordinary, that is, for configurations not complicated by major aeroelastic deformation effects or complex airframe-propulsion system interactions. Perhaps it is even true in aerodynamics that the more things change, the more they stay the same.

Concluding Remarks

Comparisons have been made of wind-tunnel-model and flight drag data for a variety of configurations representing post World War II aircraft and airplanes of the 1960's and 1970's.

The comparisons indicate that the discrepancies between the model and flight data have much in common over the time period considered, and that they primarily involve the problems caused by disproportionate boundary layers on the models (Reynolds number effects) and wall interference or blockage effects. Less prominent were sting support effects and, in the case of a large flexible airplane, the inability of the model to simulate the surface deflections for longitudinal trim.

In two instances where relatively simple, rigid, clean configurations were involved, the model-to-flight drag data confirmed the Sommer and Short T' method of extrapolating model compressible turbulent friction drag for Reynolds number effects. A unique wind tunnel-to-flight correlation of turbulent friction drag that used the same hollow cylinder in each test also confirmed the incompressible Karman-Schoenherr variation of turbulent skin friction with Reynolds number and the T' method for accounting for compressibility effects.

The major discrepancies discussed (Reynolds number effects, wall interference, and aeroelastic problems), will probably be less formidable when model testing is done in the new cryogenic tunnels. However, the 10° cone research sponsored by the U.S. Air Force and tested in flight by NASA indicates that those model tests that are affected by tunnel noise may, in some cases, require the lower disturbance level environment available in flight.

References

1. Gray, George W.: Frontiers of Flight. The Story of NACA Research. Alfred A. Knopf, Inc., 1948.

2. Nissen, James M.; Gadeberg, Burnett L; and Hamilton, William T.: Correlation of the Drag Characteristics of a Typical Pursuit Airplane Obtained From High-Speed Wind-Tunnel and Flight Tests. NACA Rept. 916, 1948.

3. Gasich, Welko E.; and Clousing, Lawrence A.: Flight Investigation of the Variation of Drag Coefficient With Mach Number for the Bell P-39N-1 Airplane. NACA ACR No. 5D04, 1945.

4. Keller, Thomas L.; and Keuper, Robert F.: Comparison of the Energy Method With the Accelerometer Method of Computing Drag Coefficients From Flight Data. NACA CB No. 5H31, 1945.

5. Carmen, L. Robert; and Carden, John R.: Lift and Drag Coefficients for the Bell X-1 Airplane (8-Percent-Thick Wing) in Power-Off Transonic Flight. NACA RM L51E08, 1951.

6. Saltzman, Edwin J.: Flight Measurements of Lift and Drag for the Bell X-1 Research Airplane Having a 10-Percent-Thick Wing. NACA RM L53F08, 1953.

7. Mattson, Axel T.; and Loving, Donald L.: Force, Static Longitudinal Stability, and Control Characteristics of a $\frac{1}{16}$-Scale Model of the Bell XS-1 Transonic Research Airplane at High Mach Numbers. NACA RM L8A12, 1948.

8. Gardner, John J.: Drag Measurements in Flight on the 10-Percent-Thick and 8-Percent-Thick Wing X-1 Airplanes. NACA RM L8K05, 1948.

9. Bellman, Donald R.; and Sisk, Thomas R.: Preliminary Drag Measurements of the Consolidated Vultee XF-92A Delta-Wing Airplane in Flight Tests to a Mach Number of 1.01. NACA RM L53J23, 1954.

10. Saltzman, Edwin J.; Bellman, Donald R.; and Musialowski, Norman T.: Flight Determined Transonic Lift and Drag Characteristics of the YF-102 Airplane With Two Wing Configurations. NACA RM H56E08, 1956.

11. Nugent, Jack: Lift and Drag of the Bell X-5 Research Airplane in the 45° Sweptback Configuration at Transonic Speeds. NACA RM H56E02, 1956.

12. Bellman, Donald R.: Lift and Drag Characteristics of the Bell X-5 Research Airplane at 59° Sweepback for Mach Numbers From 0.60 to 1.03. NACA RM L53A09c, 1953.

13. Bielat, Ralph P.; and Campbell, George S.: A Transonic Wind-Tunnel Investigation of the Longitudinal Stability and Control Characteristics of a 0.09-Scale Model of the Bell X-5 Research Airplane and Comparison With Flight. NACA RM L53H18, 1953.

14. Bellman, Donald R.: A Summary of Flight-Determined Transonic Lift and Drag Characteristics of Several Research Airplane Configurations. NASA MEMO 3-3-59H, 1959.

15. Whitcomb, Richard T.: A Study of Zero-Lift Drag-Rise Characteristics of Wing-Body Combinations Near the Speed of Sound. NACA Rept. 1273, 1957. (Supersedes NACA RM L52H08.)

16. Saltzman, Edwin J.; and Asher, William P.: Transonic Flight Evaluation of the Effects of Fuselage Extension and Indentation on the Drag of a 60° Delta-Wing Interceptor Airplane. NACA RM H57E29, 1957.

17. Beaufoy, Mark: Nautical and Hydraulic Experiments, with Numerous Scientific Miscellanies. Henry Beaufoy Press, London, 1834. (Primary source—Locke, F. W. S., Jr.: Recommended Definition of Turbulent Friction in Incompressible Fluids. DR Rept. No. 1415, Navy Dept., Bur. of Aeronautics, Res. Div., June 1952.)

18. Abbott, Ira H.; von Doenhoff, Albert E.; and Stivers, Louis S., Jr.: Summary of Airfoil Data. NACA Rept. 824, 1945.

19. Osborne, Robert S.; and Wornom, Dewey E.: Aerodynamic Characteristics Including Effects of Wing Fixes of a 1/20-Scale Model of the Convair F-102 Airplane at Transonic Speeds. NACA RM SL54C23, 1954.

20. Osborne, Robert S.; and Templemeyer, Kenneth E.: Longitudinal Control Characteristics of a 1/20-Scale Model of the Convair F-102 Airplane at Transonic Speeds. NACA RM SL54G15, 1954.

21. Sommer, Simon C.; and Short, Barbara J.: Free-Flight Measurements of Turbulent-Boundary-Layer Skin Friction in the Presence of Severe Aerodynamic Heating at Mach Numbers From 2.8 to 7.0. NACA TN 3391, 1955.

22. Peterson, John B., Jr.: A Comparison of Experimental and Theoretical Results for the Compressible Turbulent-Boundary-Layer Skin Friction With Zero Pressure Gradient. NASA TN-1795, 1963.

23. Hopkins, Edward J.; Fetterman, David E., Jr.; and Saltzman, Edwin J.: Comparison of Full-Scale Lift and Drag Characteristics of the X-15 Airplane With Wind-Tunnel Results and Theory. NASA TM X-713, 1962.

24. Saltzman, Edwin J.; and Garringer, Darwin J.: Summary of Full-Scale Lift and Drag Characteristics of the X-15 Airplane. NASA TN D-3343, 1966.

25. Quinn, Robert D.; and Gong, Leslie: In-Flight Boundary-Layer Measurements on a Hollow Cylinder at a Mach Number of 3.0. NASA TP-1764, 1980.

26. Stallings, Robert L., Jr.; and Lamb, Milton: Wind-Tunnel Measurements and Comparison With Flight of the Boundary Layer and Heat Transfer on a Hollow Cylinder at Mach 3. NASA TP-1789, 1980.

27. Pyle, Jon S.; and Saltzman, Edwin J.: Review of Drag Measurements From Flight Tests of Manned Aircraft With Comparisons to Wind-Tunnel Predictions. Aerodynamic Drag, AGARD-CP-124, Oct. 1973, pp. 25-1—25-12.

28. Arnaiz, Henry H.: Flight-Measured Lift and Drag Characteristics of a Large, Flexible, High Supersonic Cruise Airplane. NASA TM X-3532, 1977.

29. Daugherty, James C.: Wind-Tunnel/Flight Correlation Study of Aerodynamic Characteristics of a Large Flexible Supersonic Cruise Airplane (XB-70-1). I - Wind-Tunnel Tests of a 0.03-Scale Model at Mach Numbers From 0.6 to 2.53. NASA TP-1514, 1980.

30. Peterson, John B., Jr.; Mann, Michael J.; Sorrells, Russell B. III; Sawyer, Wallace C.; and Fuller, Dennis E.: Wind-Tunnel/Flight Correlation Study of Aerodynamic Characteristics of a Large Flexible Supersonic Cruise Airplane (XB-70-1). II - Extrapolation of Wind-Tunnel Data to Full-Scale Conditions. NASA TP-1515, 1980.

31. Arnaiz, Henry H.; Peterson, John B., Jr.; and Daugherty, James C.: Wind-Tunnel/Flight Correlation Study of Aerodynamic Characteristics of a Large Flexible Supersonic Cruise Airplane (XB-70-1). III - A Comparison Between Characteristics Predicted From Wind-Tunnel Measurements and Those Measured in Flight. NASA TP-1516, 1980.

32. Loving, Donald L.: Wind-Tunnel—Flight Correlation of Shock-Induced Separated Flow. NASA TN D-3580, 1966.

33. Blackwell, James A., Jr.: Preliminary Study of Effects of Reynolds Number and Boundary-Layer Transition Location on Shock-Induced Separation. NASA TN D-5003, 1969.

34. Pyle, Jon S.; and Steers, Louis L.: Flight-Determined Lift and Drag Characteristics of an F-8 Airplane Modified With a Supercritical Wing With Comparisons to Wind-Tunnel Results. NASA TM X-3250, 1975.

35. Supercritical Wing Technology—A Progress Report on Flight Evaluations. NASA SP-301, 1972.

36. Kilgore, Robert A.; Goodyer, Michael J.; Adcock, Jerry B.; and Davenport, Edwin E.: The Cryogenic Wind-Tunnel Concept for High Reynolds Number Testing. NASA TN D-7762, 1974.

37. Kilgore, Robert A.; Igoe, William B.; Adcock, Jerry B.; Hall, Robert M.; and Johnson, Charles B.: Full-Scale Aircraft Simulation With Cryogenic Tunnels and Status of the National Transonic Facility. NASA TM-80085, 1979.

38. Adcock, Jerry: Simulation of Flat-Plate Turbulent Boundary Layers in Cryogenic Tunnels. AIAA J. Aircraft, vol. 17, no. 4, Apr. 1980, pp. 284-285.

39. Usry, J. W.; and Wallace, John W.: Drag of a Supercritical Body of Revolution in Free Flight at Transonic Speeds and Comparison With Wind-Tunnel Data. NASA TN D-6580, 1971.

40. Couch, Lana M.; and Brooks, Cuyler W., Jr.: Effect of Blockage Ratio On Drag and Pressure Distributions For Bodies of Revolution At Transonic Speeds. NASA TN D-7331, 1973.

41. Dougherty, N. S., Jr.; and Fisher, D. F.: Boundary-Layer Transition on a 10-Deg Cone: Wind Tunnel/Flight Correlation. AIAA Paper 80-0154, Jan. 1980.

42. Webb, L. D.; Whitmore, S. A.; and Janssen, R. L.: Preliminary Flight and Wind Tunnel Comparisons of the Inlet/Airframe Interaction of the F-15 Airplane. AIAA Paper 79-0102, Jan. 1979.

43. Nugent, J.; Taillon, N. V.; and Pendergraft, O. C., Jr.: Status of a Nozzle-Airframe Study of a Highly Maneuverable Fighter. AIAA Paper 78-990, July 1978.

44. Plant, T. J; Nugent, J.; and Davis, R. A.: Flight-Measured Effects of Boattail Angle and Mach Number on the Nozzle Afterbody Flow of a Twin-Jet Fighter. AIAA Paper 80-0110, Jan. 1980.

45. YF-12 Experiments Symposium. Volume 3. NASA CP-2054, 1978.

46. Preliminary Analysis of STS-1 Entry Flight Data. NASA TM-81363, 1981.

TABLE 1.—SUMMARY OF WIND-TUNNEL MODEL/FLIGHT DISCREPANCIES

Aircraft	Decade	Discrepancy	Apparent cause	Remarks
P-51	Mid-1940's	Flight drag after pullout higher than for model	Different separation locations	Believe related to discussions of C-141 and M2-F3
X-5	Early 1950's	Drag difference at Mach 1, though the same at drag divergence Mach number	Chubby body, different separation locations	Probably differing afterbody flow
M-2/F-3	1960's	Base drag and boattail drag	Sting and different separation location	Compensating effects; fortuitous
X-15	1960's	Base drag	Sting-affected base pressure	Eliminated variable by subtracting out
XB-70	Late 1960's	Model drag too low at Mach 1.18*	Tunnel wall effects	Flexibility effects may also have contributed
F-8 supercritical wing	Early 1970's	2nd-velocity peak larger and farther aft in flight	Tunnel wall effects	Model too large, too close to Mach 1

*The discrepancy in the model drag data at Mach 1.18 (and 1.06) is acknowledged to represent an off-design condition; it is presented here, however, as an example of the magnitude of a transonic discrepancy in spite of a relatively modest model-tunnel blockage ratio of 0.002.

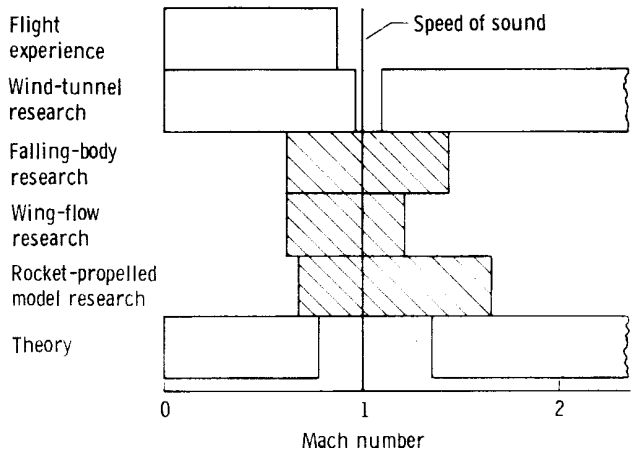

Fig. 1 The range and sources of aerodynamic knowledge as of early 1947.

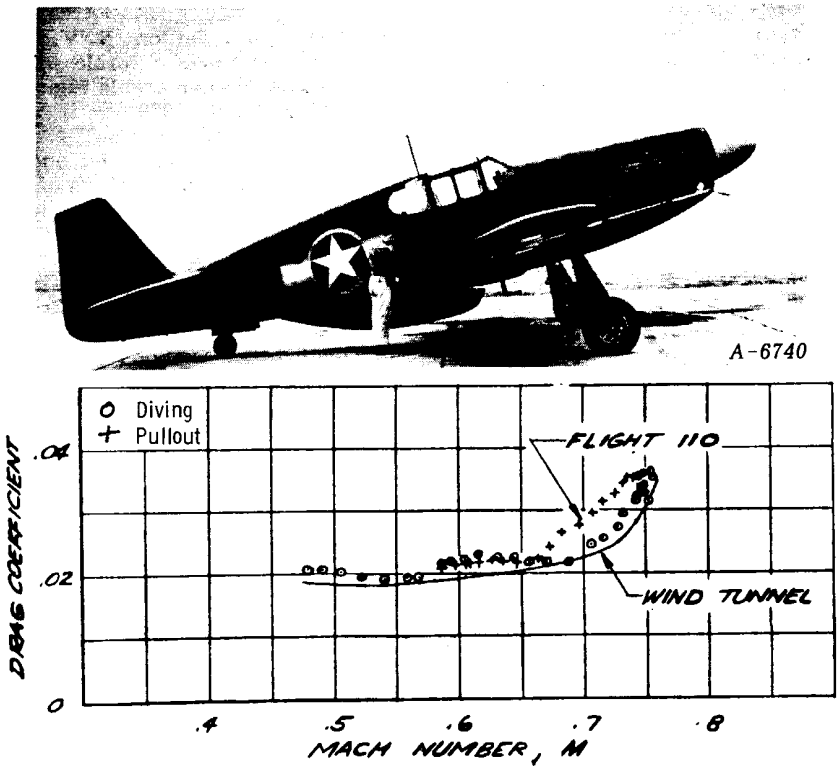

Fig. 2 Comparison of drag coefficients of the P-51B airplane as derived from flight and wind-tunnel tests.

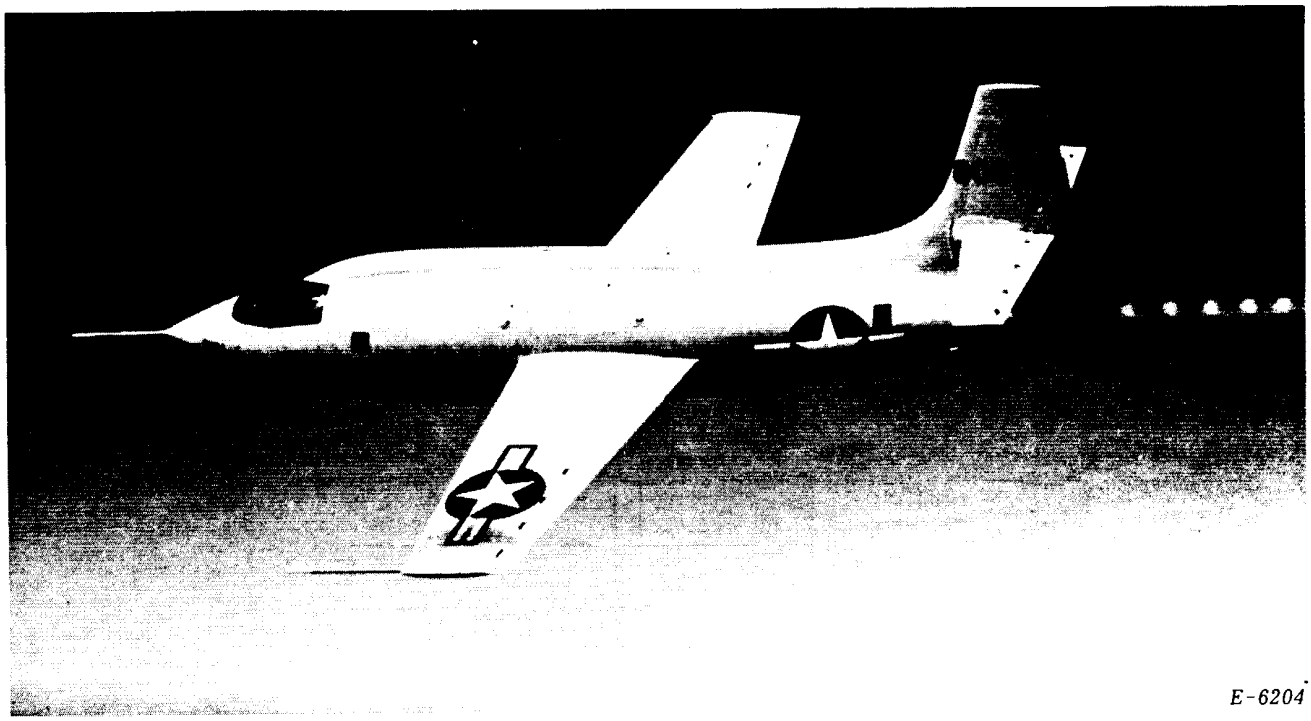

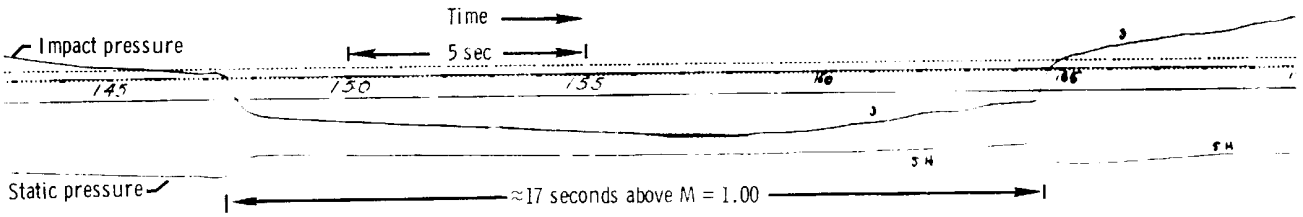

Fig. 3 XS-1 (X-1 number 1) in powered flight and historic first recorded Mach jump, Oct. 14, 1947.

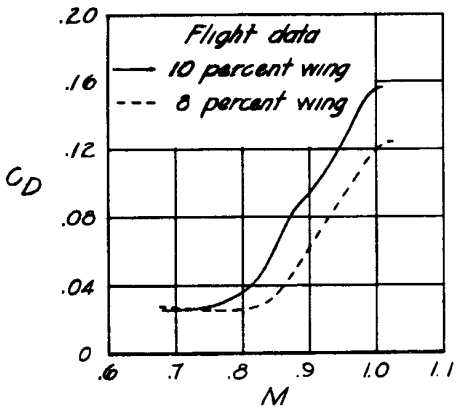

(a) Flight-to-flight comparison for t/c = 8 percent and 10 percent.

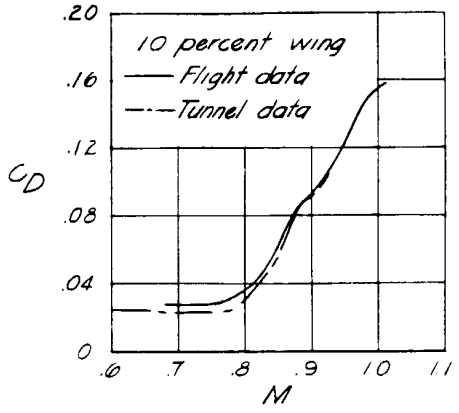

(b) Flight-to-wind tunnel model comparison for t/c = 10 percent.

Fig. 4 Variation of X-1 aircraft drag coefficient with Mach number for a constant lift coefficient of 0.4.

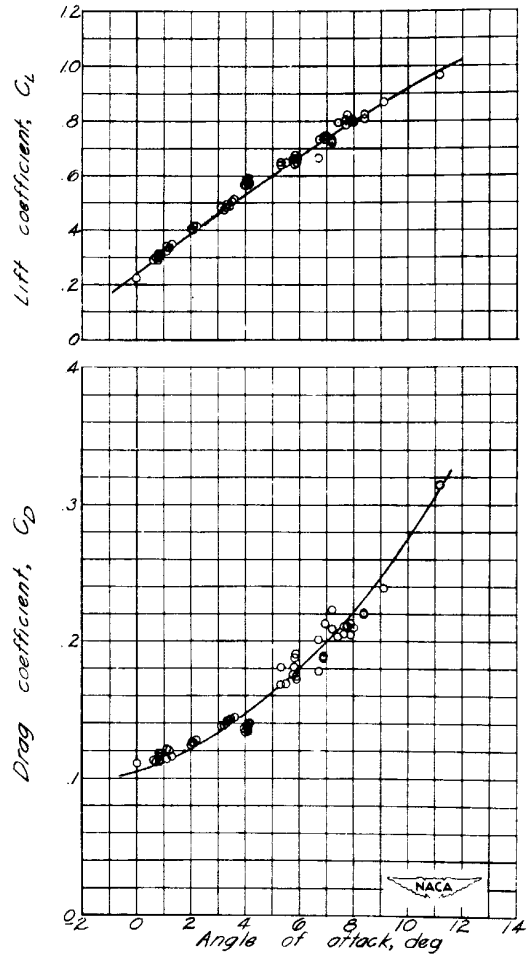

Fig. 5 The variation of C_L and C_D with angle of attack for the X-1 with the 8-percent-thick wing. M = 1.01.

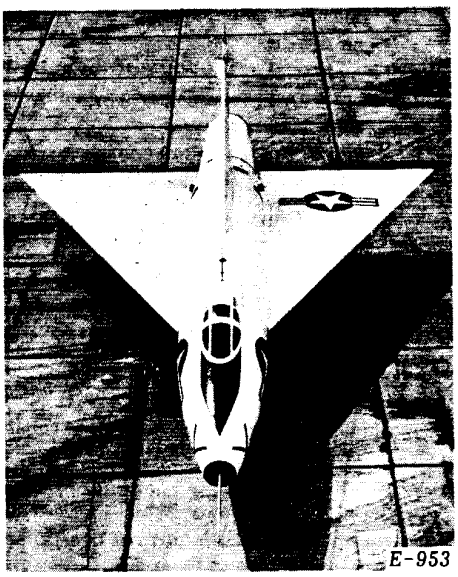

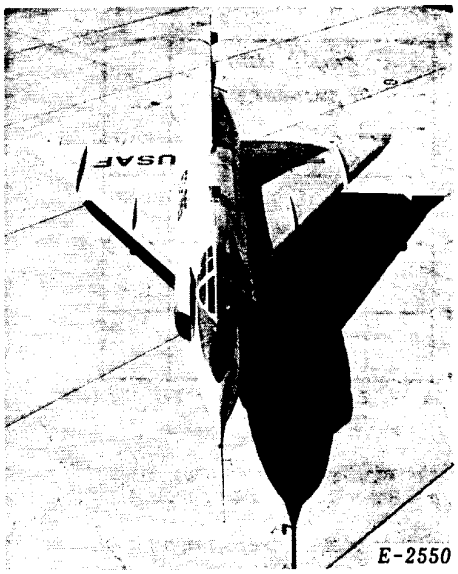

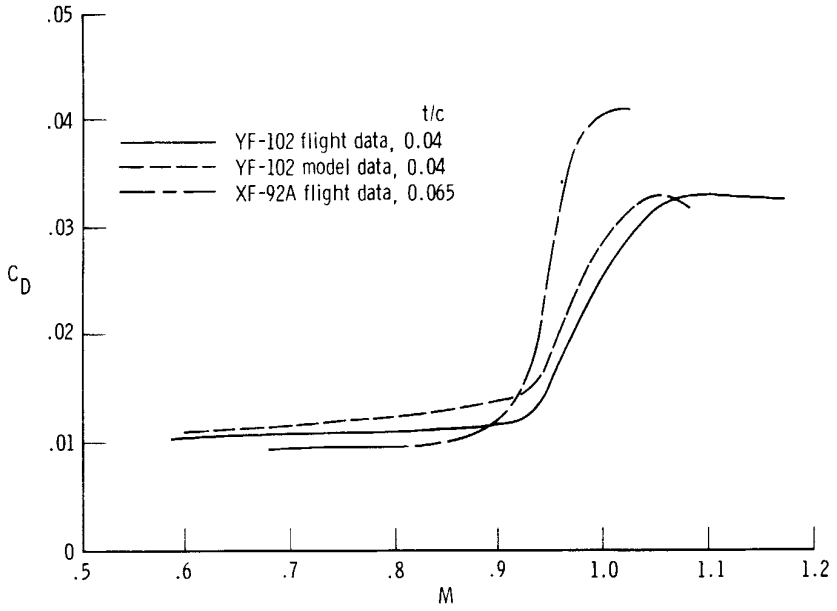

Fig. 6 Effect of wing thickness-to-chord ratio on drag divergence Mach number and the wave drag increment. $C_L = 0.08$.

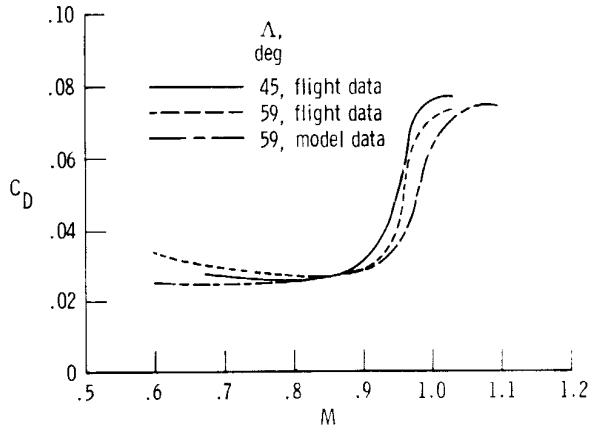

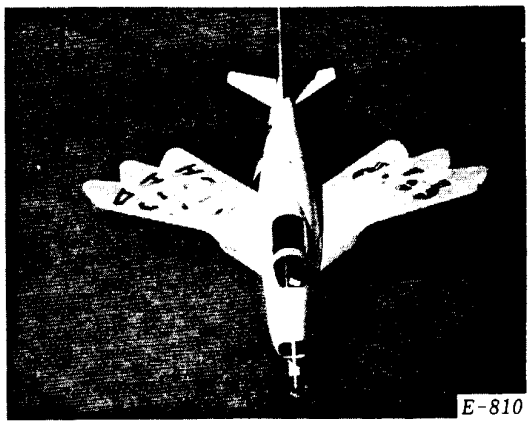

Fig. 7 Effect of wing sweep on drag divergence Mach number for X-5 airplane. $C_L = 0.2$.

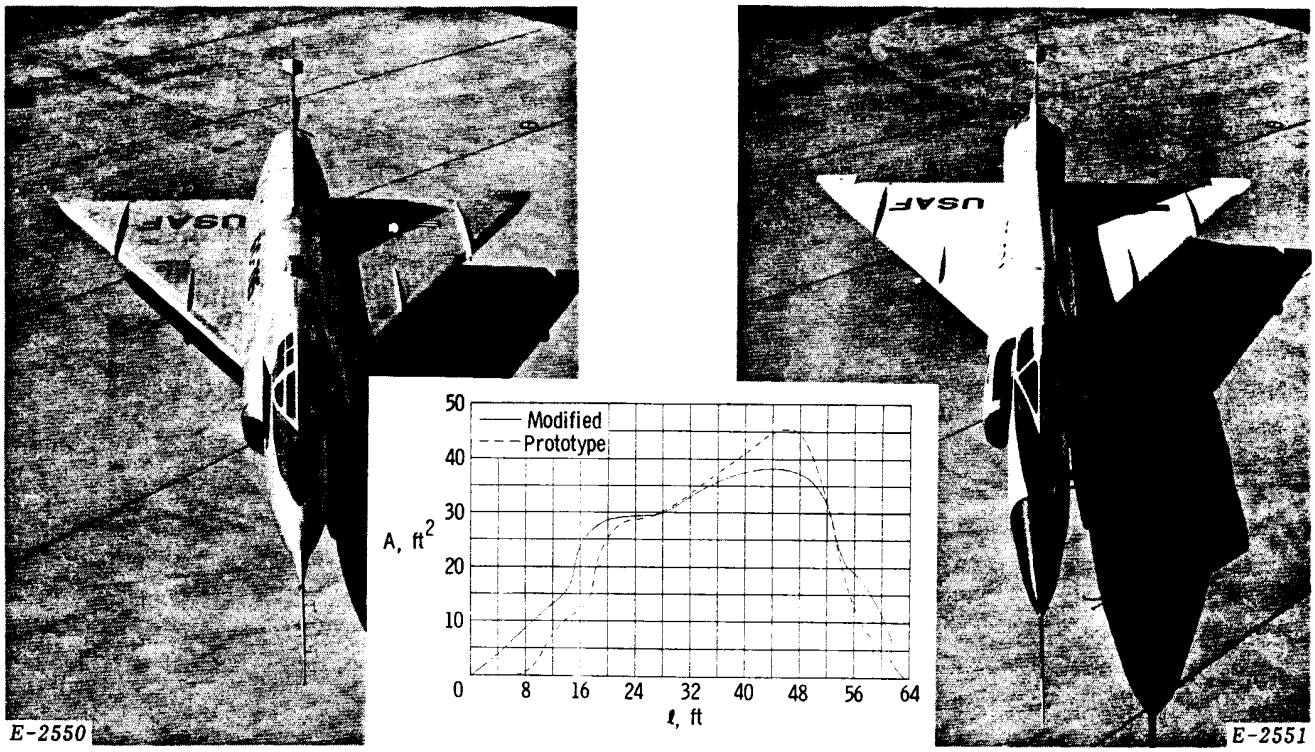

Prototype airplane, YF-102. *Modified airplane, F-102A.*

Fig. 8 Airplanes involved in full-scale transonic drag rise evaluation and the area development of each.

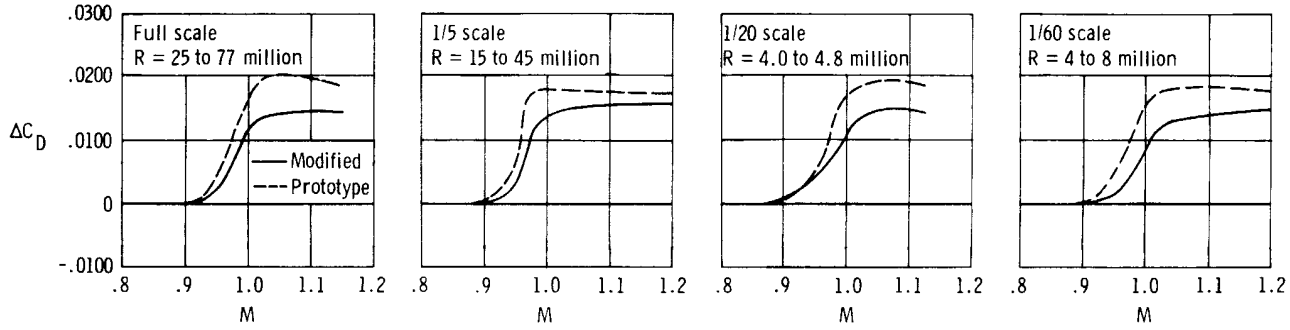

Fig. 9 Transonic drag rise characteristics of YF-102 (prototype) and F-102A (modified) full-scale configuration, 1/5-scale and 1/20-scale models, and 1/60-scale equivalent-body models.

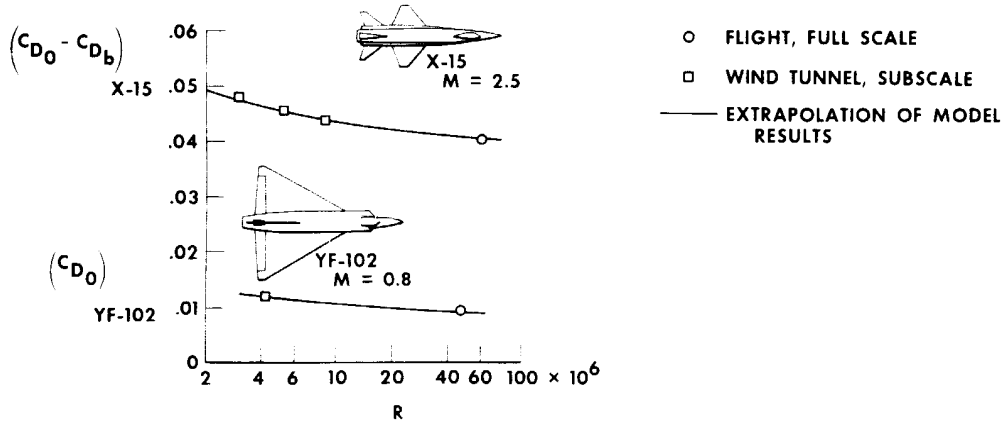

Fig. 10 Comparison of extrapolated wind-tunnel-model drag with full-scale flight results.

E-7902

10 o'clock view.

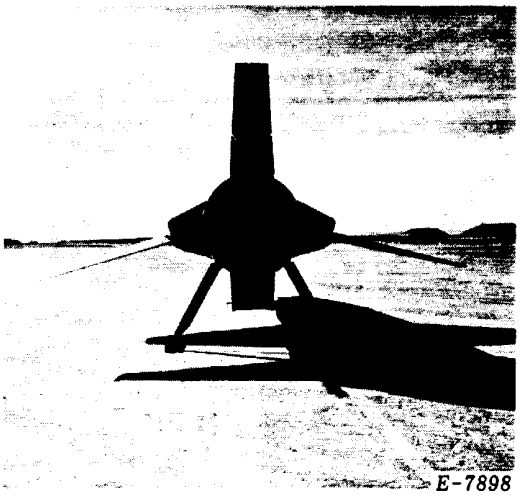

E-7898

6 o'clock view.

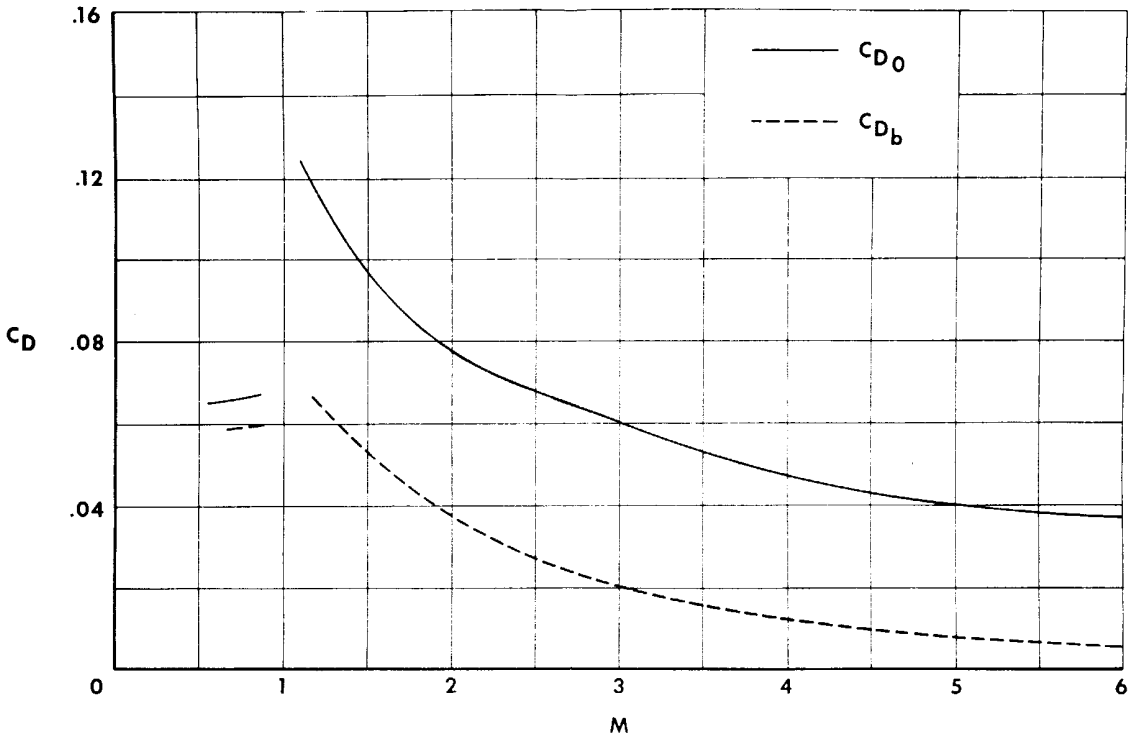

Fig. 11 Comparison of zero-lift drag and base drag for X-15. Power-off flight.

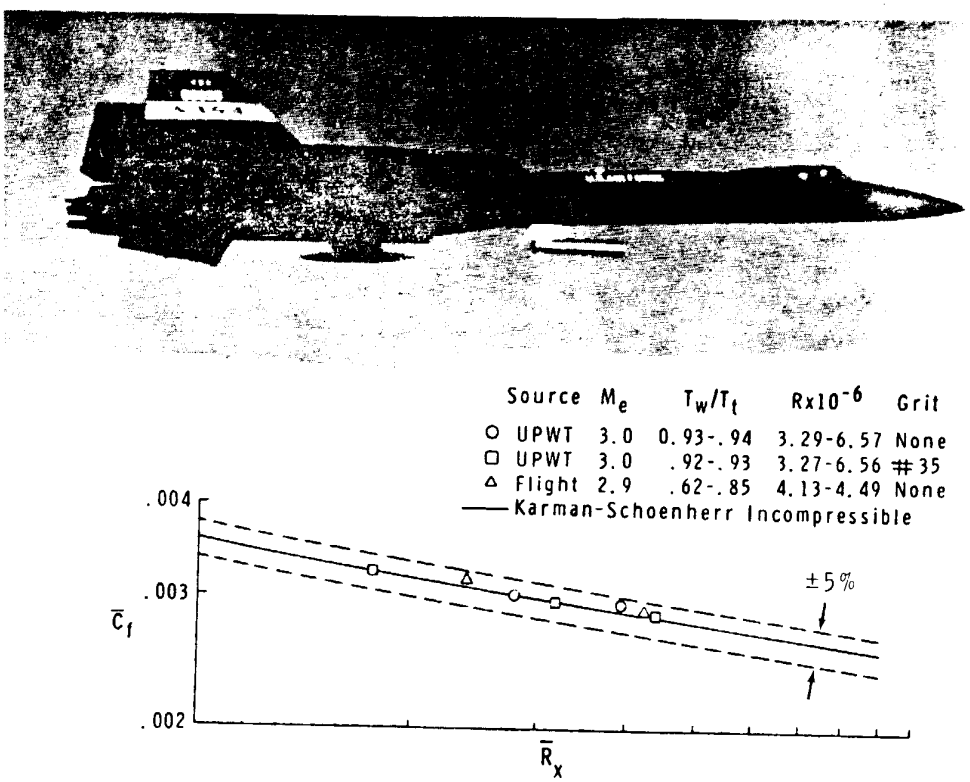

Fig. 12 Variation of local incompressible skin friction coefficient for turbulent flow with Reynolds number. T' compressibility transformation[21].

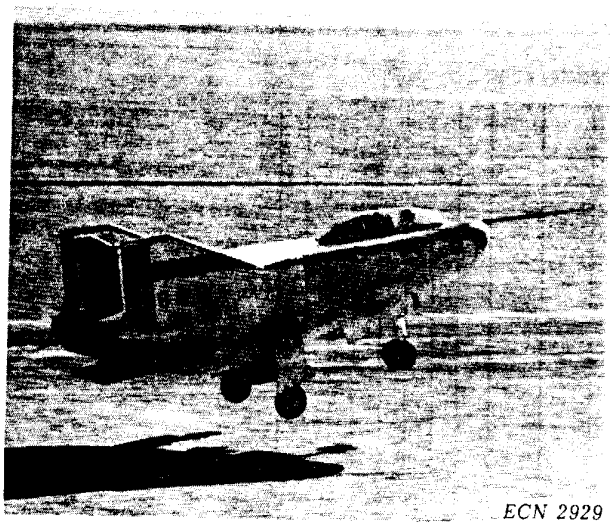

(a) M-2/F-3 prior to touchdown.

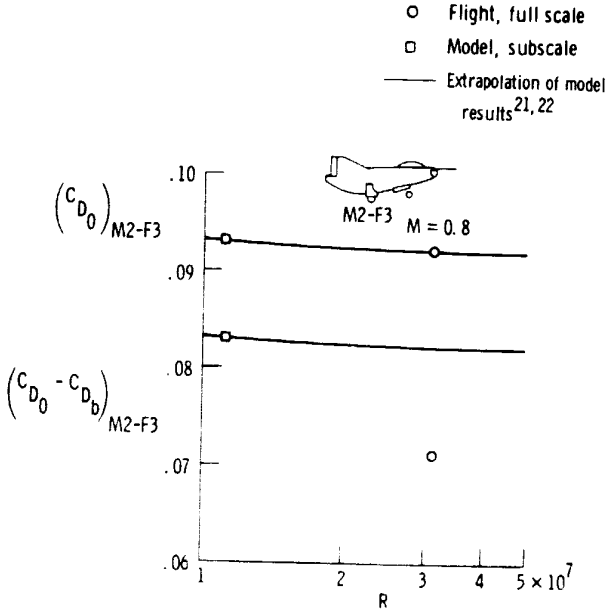

(b) Comparison of model and flight drag with and without base drag.

Fig. 13 M-2/F-3 lifting body.

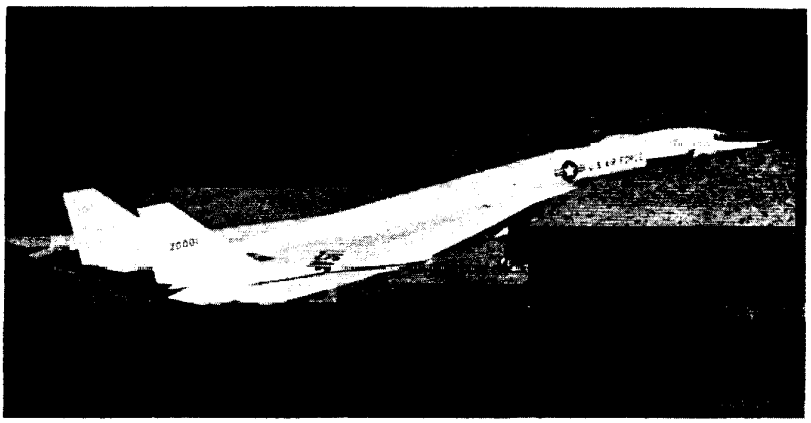

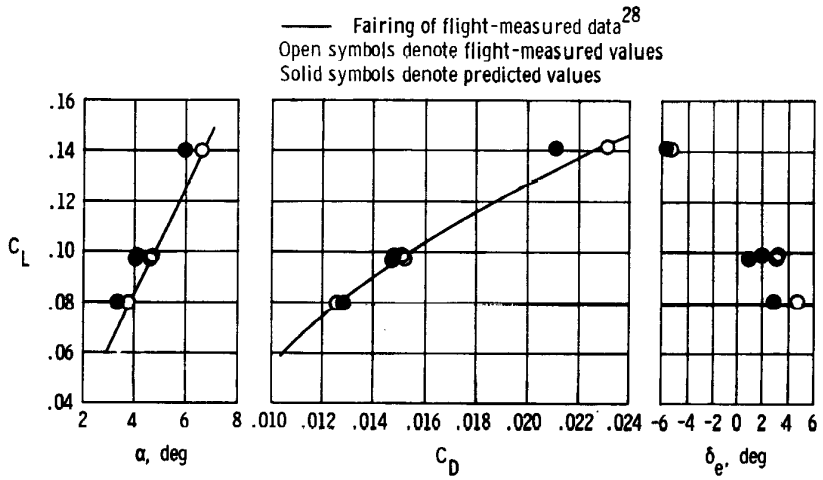

(a) $M \approx 2.5$.

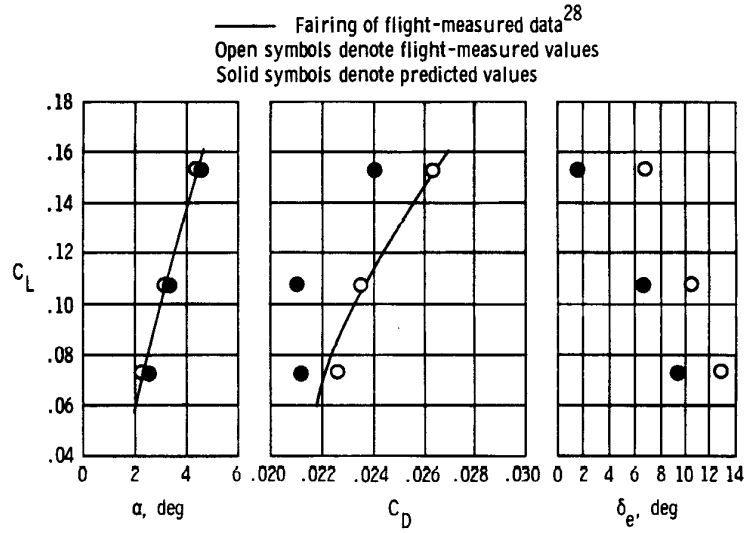

(b) $M \approx 1.2$.

Fig. 14 Lift and drag characteristics of XB-70 airplane at supersonic cruise and transonic conditions.

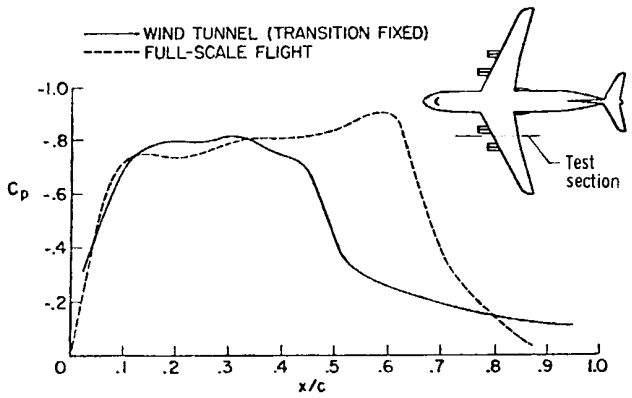

Fig. 15 Supercritical pressure distribution. $M = 0.85$.

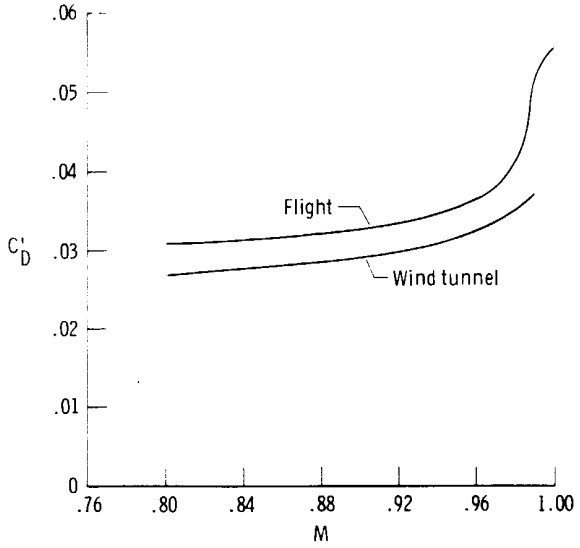

Fig. 16 Variation of drag coefficient with Mach number at design lift coefficient of 0.4.

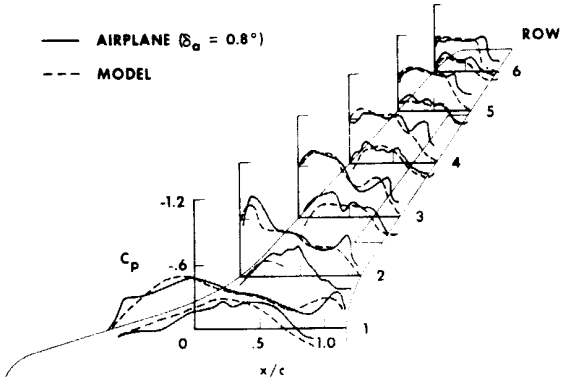

Fig. 17 Wing pressure distribution for design conditions for F-8 supercritical wing configuration. $M = 0.99$; $C_{N_{wp}} = 0.35$.

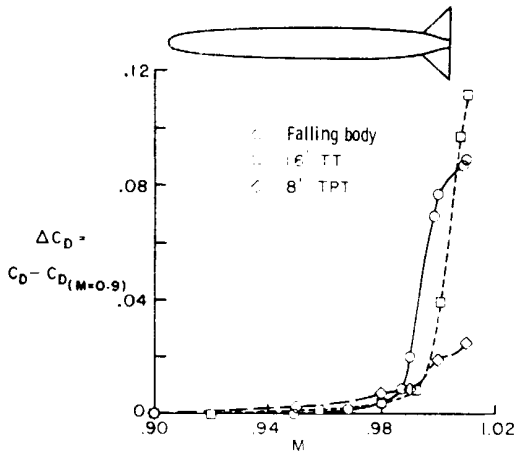

Fig. 18 Effect of wind-tunnel wall on body drag rise.

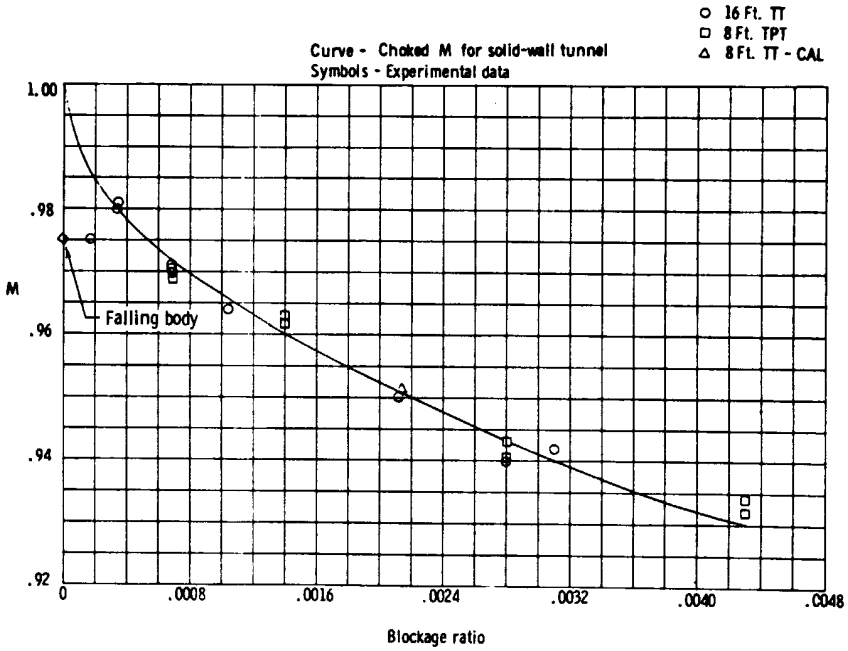

Fig. 19 Variation of transonic-creep Mach number with blockage ratio.

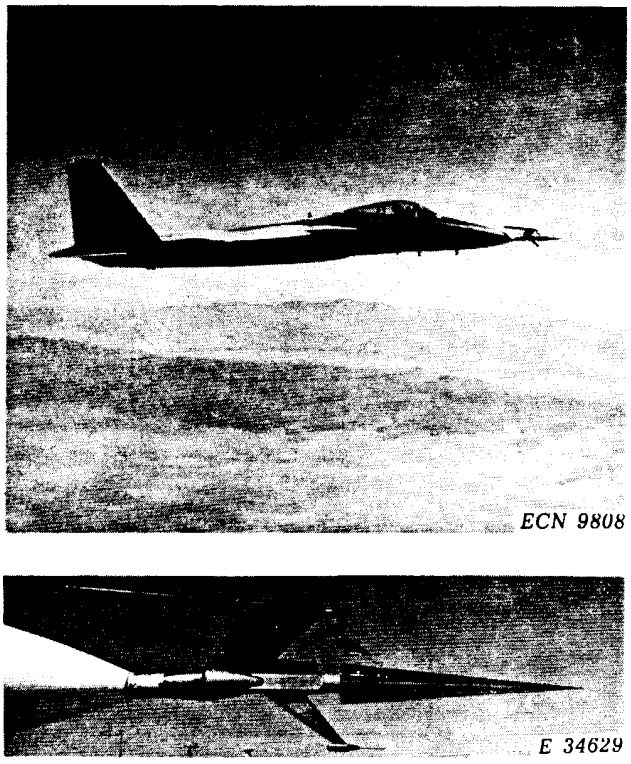

(a) F-15 airplane and 10° cone.

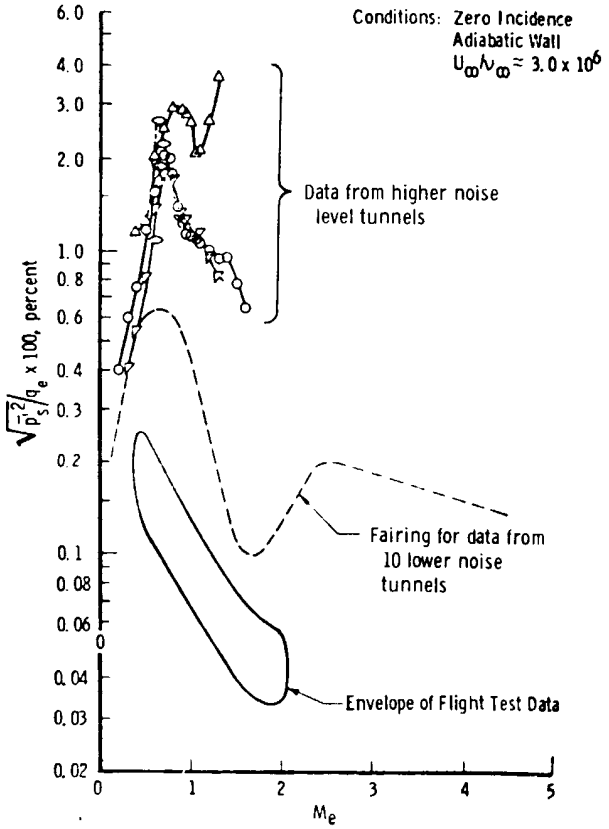

(b) Comparison of disturbance levels measured in wind tunnels with disturbances in flight.

Fig. 20 Summary of results from 10° cone experiment.